ISSN: 1311-1728 (printed version); ISSN: 1314-8060 (on-line version)

DEVELOPMENT OF A TRANSPARENT ULTRA-THIN ANTENNA FOR **SUB 6 AND C BAND COMMUNICATIONS**

¹Jyothi Bandarupalli, ²Sreevardhan Cheerla, ²Boddapati T P Madhav, ¹Yalavarthi Usha Devi

¹Research Scholar, KLEF, ECE Department, Guntur DT. Andhra Pradesh, India. ²ALRC-R&D, KLEF, ECE Department, Guntur DT. Andhra Pradesh, India Mail ids: jyothicnr@gmail.com, sreevardhancheerla@kluniversity.in, btpmadhav@kluniversity.in, ushadevi.yalavarthi@kluniversity.in

Abstract

A transparent ultra-thin antenna developed for mid band 5G and C-band frequencies is presented. This antenna has been engineered to operate effectively across three distinct frequency bands catering to eMBB, WIFI, and C band applications. The antenna design comprises a rectangular patch in which rectangular, circular, and semicircular slots are introduced. The ultra-thin model is realized on one side ITO-coated PET sheet as a substrate with dimensions 16x16x0.175 mm³. The ITO-coated side of the PET sheet acts as ground and the patch is realized using silver conductive paste. It operates at two bands namely 2.8 GHz and 4.9 GHz in the sub 6 region and a wide band ranging from 7.3GHz to 8.3GHz in the C band. This Model is optimized to operate effectively across these three distinct frequencies with a maximum impedance bandwidth of 12.82%. The maximum gain obtained is 3.81db at 7.5GHz. The antenna uses transparent materials to balance functionality with architectural compatibility facilitating its integration into existing environments. Experimental results confirm that the antenna matches all three bands impedance. In addition to fulfilling the demand for multifunctional antennas in compact electronic systems, this work facilitates to the improvement of seamlessly integrated wireless technologies within everyday objects.

Index Terms: eMBB, Transparent antenna, ITO.

I. Introduction

Due to proliferation of wireless technologies, there is a growing emphasis on designing hardware that combines compactness, cost efficiency and multi-functional performance with ease of integration [1]. On a larger scale wireless communications have taken place by means of large, and often unsightly antennas [2]. These antennas are often bulky and visually intrusive. Whereas, transparent antennas are designed specifically to be nearly invisible and seamlessly integrate into almost all the surfaces including solar panels, Windows, screens and also wearable devices. This transparent design strategy supports both aesthetic compatibility and functional adaptability, making it suitable for discreet 5G network integration in urban infra structure. As 5G technology continues to evolve the role of transparent antennas is expected to be increasing significantly offering a practical solution for the deployment of high

Received: July 21, 2025 438

Volume 38 No. 1s, 2025

ISSN: 1311-1728 (printed version); ISSN: 1314-8060 (on-line version)

speed, low latency networks in densely populated areas. For immersive applications the use of transparent antennas is gaining momentum as a means to mitigate size constraints and enable more adaptable design configurations [3]. Other applications where transparent antennas are used include vehicular communications [4]-[7], satellite communications [8]-[11], Internet of things [12]-[15] etc. A circularly polarized transparent antenna for vehicular communications operating in two bands is proposed in [4]. The size of the antenna is 180X180X5 mm³ whose gain is given by 2.2 dBic and 3.8 dBic for the two bands and the efficiency for both the frequency bands varies approximately from 55-75%. In [5], a transparent antenna for vehicular communications is presented with glass as substrate and the overall dimensions are 50 X 17 X 1.1 mm³. The maximum gain obtained is negative with radiation efficiency under 15 %. A transparent wide band CPW fed circularly polarized antenna is presented in [6], with dimensions of 149 X 99 X 1 mm³. It has a gain of 5.3dbic and its efficiency is not mentioned. [7] presents a monopole antenna attached on the glass of a vehicle whose dielectric constant is given by 6.95 and is 3.2 mm thick. The foot print of the antenna is given by 50X50 mm ² and its maximum gain is given by 5dbi. A highly efficient Ka band transparent reflect array antenna for satellite communications is presented in [8]. The size of the aperture is given by 160 X 150 mm² with an efficiency of 40% and is of gain 27.3 dbi. Combination of active integrated antenna and an optically transparent reflect array resulted in gain enhancement for cube sat applications [9]. In this paper a gain of 22.7 dB is improved by using active integrated antenna (AIA) approach and it is further improved by using transparent reflect array. Thus, giving a high gain of 42.3 dB for the fabricated model. The footprint of the antenna is given by 110 X 80 mm². On the top surface of the solar cell, an antenna was designed and fabricated [10], showing super wide band characteristics. Initially the antenna was designed over 1.6mm thick FR4 substrate. Then it has been changed to plexi glass of thickness 1mm to achieve transparency. No noticeable change is observed in the bandwidth by using plexi glass. Also, the antenna is of compact size given by 29 X 27 X 1 mm³. Its peak gain and efficiency are given by 8.1 dB and 90% respectively. A sub array antenna based on solar panel with two substrates maintaining optical transparency for CubeSat application is proposed in [11]. The substrate at the bottom is TMM 10i of 0.762 mm thickness and the substrate on the top is transparent PET G of thickness 2mm. Energy harvesting is done by placing the solar panel between the two substrates. Even though the bottom substrate is not transparent, it makes no difference as it is placed under the solar panel. For the top substrate a thin film of optically transparent conductor is used as a patch. Further, an improvement in directivity is obtained by the use of a reflective surface layer having circular FSS unit cells that are identical. Maximum gain of the proposed model is given by 16 dB at the operating frequency 10 GHz and its efficiency is greater than 65%. A transparent UHF-RFID tag antenna is proposed for seamless integration into smart city IoT applications in [12]. This design utilizes a 3mm thick corning glass substrate achieving 37% radiation efficiency and -2.1 dBi gain. The reason behind relatively low radiation efficiency is mentioned as the high dielectric loss of the glass substrate and high conductive loss of the ITO film. For enhanced long-term comfort and wearability, optical transparency has been identified as beneficial in epidermal electronic applications [13].

Volume 38 No. 1s, 2025

ISSN: 1311-1728 (printed version); ISSN: 1314-8060 (on-line version)

In this context, a transparent epidermal antenna tailored for inconspicuous, human centric IOT applications is introduced. This antenna with dimensions of 75 X 45 mm² demonstrates up to -12.6 dBi realized gain and a radiation efficiency of 2.32 %. In another IoT focussed work, a double folded loop antenna was fabricated on a 0.5mm thick transparent poly carbonate substrate. The foot print of the model is given by 43 X 36 mm² and has a realized gain of over -6.2 dbi for the transparent conductor at 2.4 GHz. Similarly, another antenna which is optically transparent and is intended for IoT use was reported in [15], utilizing a 0.04mm thick acrylic sheet substrate sized at 220mm X 80 mm. The antenna displayed a peak gain variation of up to 0.1 db. For wireless LAN and mid band 5G communications, a CPW fed transparent antenna employing PET substrate was detailed in [16]. This design, measuring, 78 X 58 X 0.9 mm³ displayed an average gain of 3 dBi and the efficiency is reported to be 80%. Transparent microstrip patch antenna is made using transparent conductive film in [17]. It was fabricated using different conductive materials like multi-layer film, multi metal film and copper sheet on a transparent acryl substrate. Then, a performance comparison is made in terms of peak gains and radiation efficiencies. The dimensions of the model are given by 50X50X1 mm³. When multi-layer film is used for conductive part, the maximum gain is -4.23 and its radiation efficiency is given by 7.76% respectively. The maximum gain and radiation efficiency values, 2.63 dB and 42.69% respectively, were achieved using multi mesh film. An ultra-wideband monopole antenna that is optically transparent is proposed in [18] for energy harvesting in solar applications. The physical dimensions of the proposed model are given by 50mm X 50mm x 1.1 mm. In this work multi film approach is used to improve the gain. By using this, the peak gain is improved from -8 dBi to 5 dBi. In [19] gold nano deposition is proposed as an effective technique for improvement in the performance of radiation efficiency of a transparent antenna. Here DC sputtering is used to deposit gold nano layer. The maximum gain obtained is -8dBi at 4 GHz and the footprint of the proposed model is 50 X 50 mm². A wearable compatible antenna featuring both transparency and flexibility has been developed in [20]. A multi-layer electrode film is used as conductor for the presented antenna. This antenna measuring 54 X 36 mm² exhibits 40% average efficiency and gain of up to 4dBi between 2.4 – 2.5 GHz band. In [21], a wideband, flexible and transparent antenna was introduced to support both mid band 5G and wireless LAN applications. This design, incorporates melinex substrate and employs AgHT-4 as transparent conductive material. The antenna measures 30 X 20 mm² achieving a gain of up to 0.53 dBi and its efficiency has a minimum value of 41%. Another study [22] showcases microstrip patch antenna constructed using transparent substrate and fluorine doped tin oxide as conductor. Mounted on a borosilicate glass substrate measuring 100 X 80 mm², the antenna delivers 1.72 dB gain and operates with 33.27% radiation efficiency. [23] presents a dual polarized antenna using transparent materials designed for 5G mid band usage. It utilizes a stacked configuration comprising of two polycarbonates layers each 50 X 50 mm² in size with a dielectric constant of 2.7. The upper surface includes a parasitic patch of square shape with integrated parasitic strips and slots of T shape. The sheet resistance of transparent conductive mesh material used for all conductive parts is 0.09 Ω /sq. 4.14 dBi of measured gain is reported for this model. Transparent monopole antenna, proposed in [24] for WiMax applications is

Volume 38 No. 1s, 2025

ISSN: 1311-1728 (printed version); ISSN: 1314-8060 (on-line version)

utilizing AgHT-4 for the conductive parts. Fabricated on a 2mm thick glass substrate with dimensions of 90mm X 60 mm, this model achieves 3.16 dBi gain.[25] introduces monopole transparent antenna used in WCDMA and wireless LAN applications with a prototype fabricated using PET sheet of size 30mm X 30 mm² as substrate. ITO film is used for conductive parts which is deposited by magnetic sputter. In [26], the performance of monopole antennas using different transparent conductive materials such as ultra-thin copper, indium tin oxide (ITO) and ITO/Cu/ITO multi-layers is evaluated. Here Ground plane is made by using a rectangular brass plate of size 150 X 150 mm². Also the gain of the antenna when ITO layer is used as a conductor is given by -4.10 dBi. [27] explores a transparent patch antenna aimed at enhancing gain as well as efficiency. It employs TCF coated PET film of thickness 0.2mm, supported using a 2 mm thick curved pet g frame. The patch width is 50 mm with a substrate extension of 75 mm. Simulation results for the flat version show an efficiency range of 9-18% with gains between -2.7 to 0.5 dBi. Notably the curved configuration significantly improved performance reaching a maximum gain of 2.57 dBi and the value of efficiency lies between 41-44%. A practical and efficient method is proposed to enhance the performance of the antennas using TCF. In this approach, a supportive dielectric is constructed using polyethylene terephthalate glycol (PETG) with a thickness 2 of mm. This frame holds a curved PET film of 0.2mm thickness, which is has a TCF layer coated on the upper side. The width of the patch is 50 mm while the substrate extends up to 75 mm. For the flat configuration, the simulated adiation efficiency ranges from 9 to 18%, whereas its gain ranges from -2.7 to 0.5 dBi. When reshaped into a curved structure, the antenna exhibits a notable improvement in performance achieving 2.57dBi gain along with radiation efficiency in the range 41-44 %. In [28], an "antenna on display" was implemented using an ultra-thin substrate to support sub 6 GHz wireless communication. The antenna design attained 2.67 dB maximum gain along with 69.9% radiation efficiency, showcasing its suitability for integration into transparent or display based electronics. Additionally, a high efficiency optically transparent monopole antenna was fabricated using a silver grid layer offering improved radiation characteristics while maintaining optical transparency in [29]. This approach demonstrates the potential of metallic mesh patterns for achieving both electrical performance and visual discretion in antenna systems. Here two monopole antennas have been fabricated, one is non-transparent designed for comparison with transparent mono-pole constructed using meshed bilayer made of Ag/Ti. These monopoles of dimensions 50 X 50 mm², were laid down on a ground plane of rectangular shape with dimensions 600mm X 600 mm. The obtained gain of the transparent monopole has a maximum value of 2.24 dB and its efficiency is given by 85%. A flexible, compact and transparent antenna incorporating a metallic mesh was presented in [30] for use in 5G wearable technologies. The antenna measuring 60 X 60 mm², attained a gain of 3.8 dBi and an efficiency of up to 85% at 4.8 GHz and 5 GHz respectively, emphasizing its suitability for integration into body-worn devices. In [31], an innovative method was proposed to improve performance of transparent film antennas by introducing a narrow strip of highly conductive material at locations with high current concentration. This design utilizes a conductive AgHT coated film of size 120 X 60 mm² and the implemented method improved efficiency from 38% to 68 %

ISSN: 1311-1728 (printed version); ISSN: 1314-8060 (on-line version)

with a corresponding gain enhancement from -5 dBi to 0 dBi. In [32], a comprehensive study is conducted on transparent microstrip antennas constructed using fluorine doped tin oxide (FTO)films, which were deposited using the spray pyrolysis method. The study includes the development and comparison of antennas with fully transparent patch and ground planes against conventional copper-based counter parts. The antenna utilizing both transparent components recorded, 1.72 dBi gain at 5 GHz frequency and a maximum efficiency of 33.27 %. Thus, transparent antennas are widely used in various applications as discussed so far. Still there is an emerging need for a compact and flexible transparent antenna that operates in different frequency bands.

The primary focus of this paper is to implement a compact rectangular microstrip antenna that operates effectively within both the mid band 5G and C band spectra. The designed antenna is also optimized by the use of HFSS simulation platform. To ensure flexibility and transparency, the structure is realized on a single layer PET substrate. This work makes the following significant contributions:

- 1.A low profile microstrip patch antenna on transparent PET substrate is modelled and optimized using HFSS simulation software.
- 2. Step by Step Design methodology is done to obtain desired frequency bands.
- 3.Performed bending analysis to test flexibility of the model.
- 4. Fabricated the model using one side ITO coated PET sheet and the patch is realized with silver conductive paste.
- 5. The fabricated model is tested with VNA and results are compared with simulation.

II. Antenna Geometry

The proposed model uses 0.175 mm thick PET material characterized by a relative permittivity of 3 and 0.002 value for loss tangent, as substrate. The substrate measures 16X16 mm ² while the radiating patch is sized at 12X11mm². It is fed by a microstrip line. Figure 1 presents the proposed design's layout, with table 1 outlining the corresponding geometric parameters.

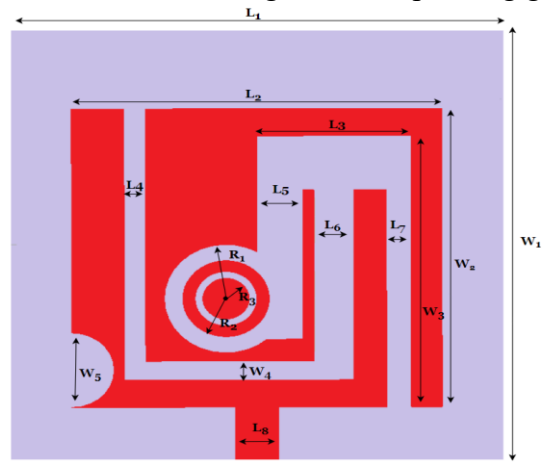


Fig 1: Schematic diagram of the final transparent model

ISSN: 1311-1728 (printed version); ISSN: 1314-8060 (on-line version)

Symbol	Dimension(mm)	Symbol	Dimension(mm)
L ₁ (c)	16	W1(d)	16
L ₂ (a)	12	W2(b)	11
L ₃	5	W_3	9
L ₄	0.7	W_4	0.7
L ₅	1.5	W 5	1.375
L ₆	1.3	\mathbf{R}_1	2
\mathbf{L}_{7}	0.8	R ₂	1.4
L ₈	1.4	R ₃	0.75

Table 1: Geometric parameters of the proposed transparent antenna

The antenna design methodology is illustrated in figure 2 starting with a simple slotted rectangular patch. In the first step, a fundamental rectangular structure incorporating a single slot is analysed to evaluate its initial performance characteristics. It resonated between 8.6 GHz to 8.8 GHz. Two more slots are introduced in step 2 which resulted with an extra band from 7.2GHz to 7.3 GHz. By introducing another rectangular slot in contact with these slots, two bands one at 4.1GHz and the other from 7.6 GHz to 7.7 GHz is observed in step 3. Later one more slot is introduced which is not in connection with the first three slots in step 4. This configuration produced dual band operation at approximately 3 GHz and 5.1 GHz. In step 5, a rectangular slot was introduced to connect the previously placed slots resulting in the excitation of three distinct frequency bands: 3 GHz,6.2 GHz, and 8.2 - 8.4 GHz. Subsequently in step 6, the addition of a circular slot further increased the number of resonated frequencies to 4, occurring at 2.8 GHz, 5 GHz, 7.3 - 7.8 GHz and 8.1 - 8.3 GHz.

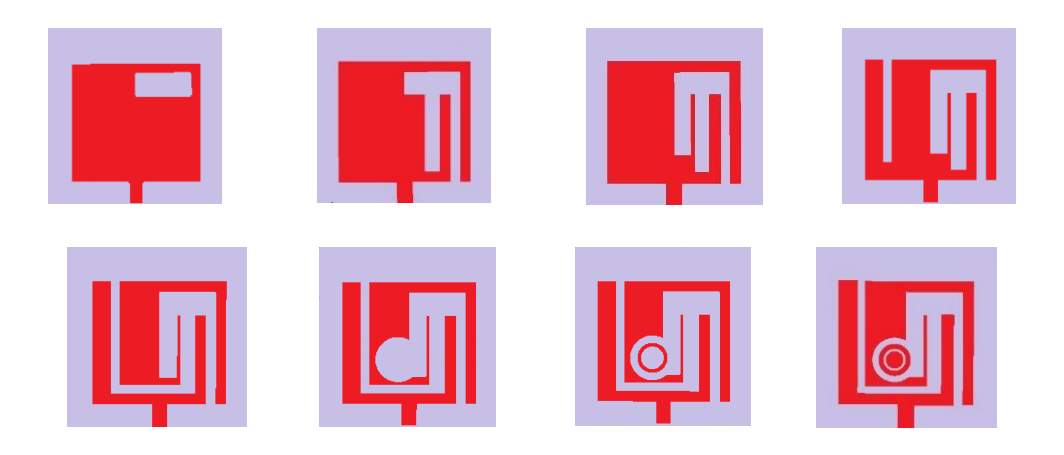


Figure 2: Step by Step analysis

Steps 7 and 8 involved adding circular patches inside the circular slot mentioned in step 6. The antenna model developed in Step 7 exhibits resonant frequencies at 2.8 GHz,5.1 GHz,7.5-7.7 GHz and 8.2 - 8.4 GHz. And the design evolved in step 8 resonated at 2.8GHz,4.9 GHz, 7.2

ISSN: 1311-1728 (printed version); ISSN: 1314-8060 (on-line version)

GHz, and 8.2 GHz. The Indium Tin Oxide coated at one side of the PET substrate acts as ground while the radiating patch is formed using silver conductive paste. The antenna structure incorporates both circular and rectangular slots to achieve the desired multi band performance.

III. Results and Discussions

Figures 3 and 4 depict the simulated reflection coefficient across different frequencies for the intermediate antenna configurations generated during design stages 1 to 8. In figure 3, representing steps 1-4, the reflection coefficient plots reveal resonance at multiple bands including 3GHz,4.1GHz, 5.1 GHz,7.2 – 7.3 GHz,7.6 – 7.7 GHz and 8.6 – 8.8 GHz covering sub 6 GHz frequency range. Figure 4 presents reflection coefficient characteristics for models in steps 5-8. Initially, the designs resonated at two distinct bands. However, the addition of rectangular slot in step 5, introduced a third resonance demonstrating improved spectral utilization. In steps 6 through 8 circular slots and parasitic patches were incorporated. This led to the emergence of distinct resonant bands located at 2.8 GHz,4.9 GHz,5.1 GHz,7.2 GHz,8.2 GHz, 7.3 GHz to 7.8 GHz, 7.5 GHZ to 7.7 GHZ, 8.1 GHz to 8.3 GHz and 8.2 GHz to 8.4 GHz. These enhancements indicate the effectiveness of slot loading in tuning antenna resonances and they establish models' utility across sub 6 GHz and C band spectra. The final proposed model was developed by introducing semicircular slot to the optimized structure from step 8. As shown in figure 5 it resulted in two well matched resonance bands at 2.8 GHz and 4.9 GHz both within sub 6 region and wider operating band spanning from 7.3 GHZ to 8.3 GHz suitable for C band 5G and WLAN applications. These results confirm that the proposed model offers multi band operation, excellent impedance matching, and sufficient spectral separation for modern wireless communication standards.

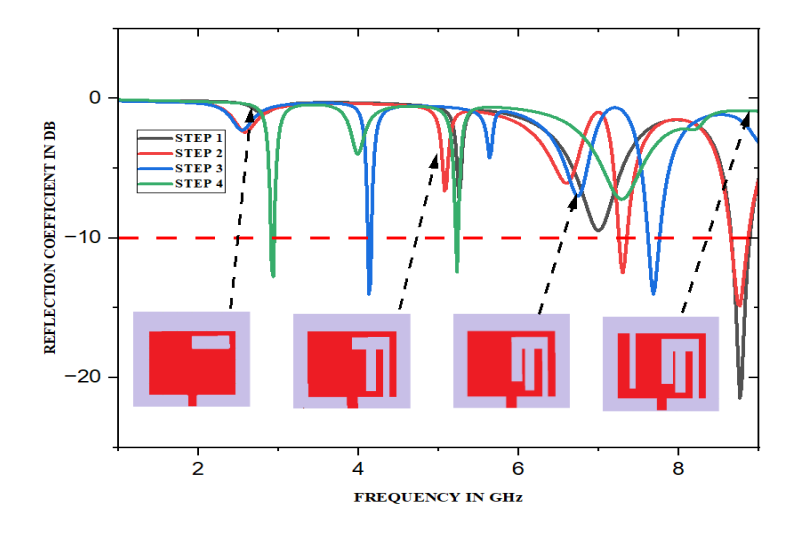


Fig 3:Steps 1-4 with their simulated reflection coefficient.

Volume 38 No. 1s, 2025

ISSN: 1311-1728 (printed version); ISSN: 1314-8060 (on-line version)

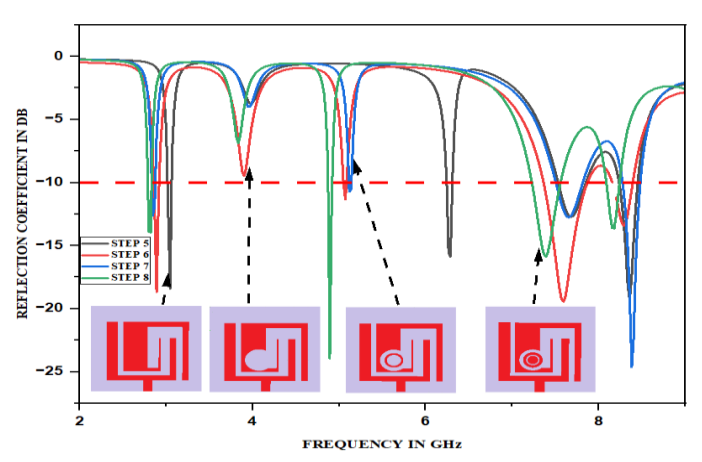


Fig 4: Steps 5 - 8 with their simulated reflection coefficient.

The field plots illustrating simulated electric field and magnetic field distribution of the proposed model are presented in figure 6.

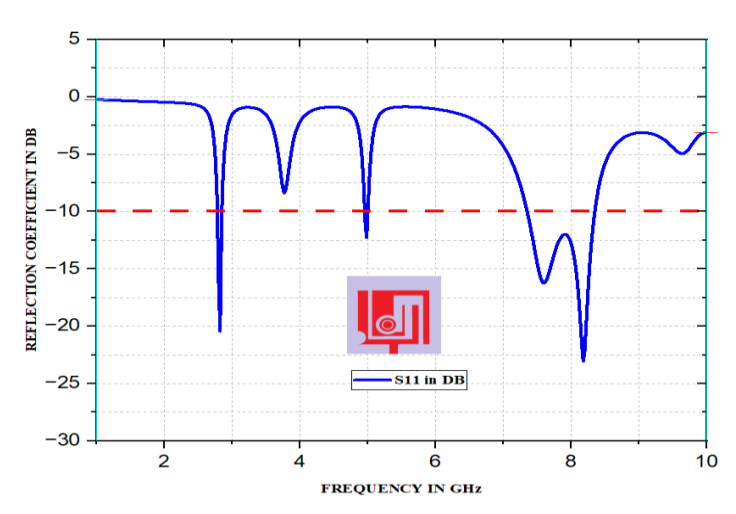
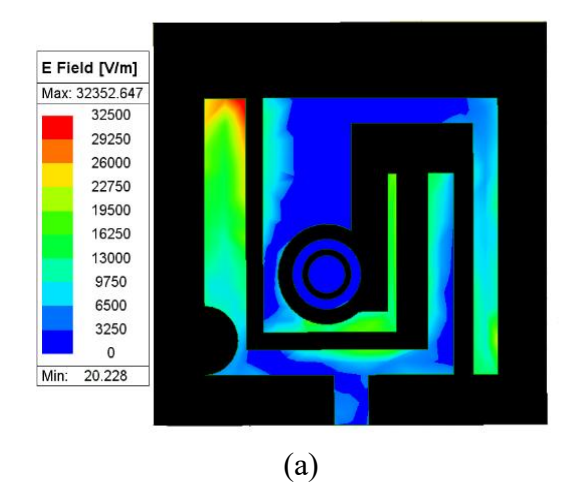


Fig 5: Reflection coefficient variation with frequency of the final structure



Volume 38 No. 1s, 2025

ISSN: 1311-1728 (printed version); ISSN: 1314-8060 (on-line version)

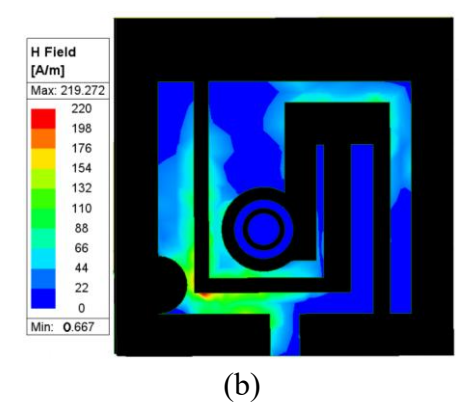


Fig 6: (a) Simulated Electric field distribution of the proposed model, (b)Simulated Magnetic field distribution of the proposed model

Figure 7 shows the simulated radiation efficiency of the developed design. A maximum radiation efficiency of 69.9% has been observed at 7.4 GHz.

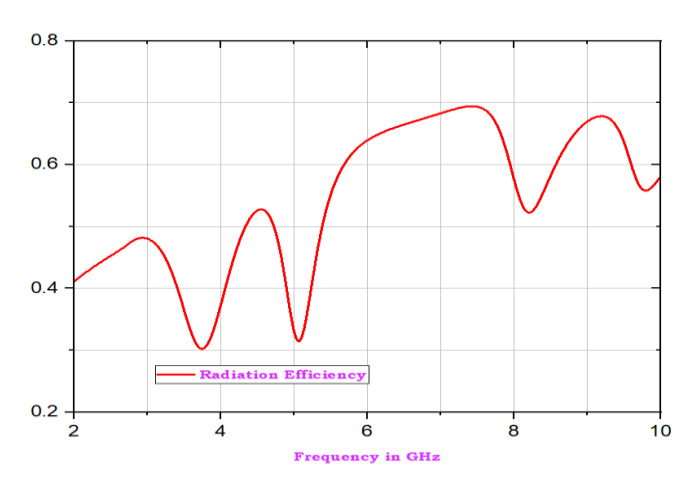
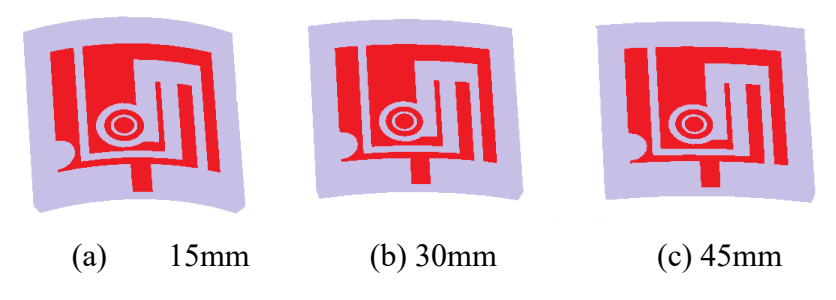


Fig 7: Radiation efficiency of the proposed model

The resilience of the developed design has been simulated by subjecting it to various bending radii along the horizontal and vertical component. Figure 8 displays the antennas bending behaviour along Y axis and X axis at various radii.



ISSN: 1311-1728 (printed version); ISSN: 1314-8060 (on-line version)

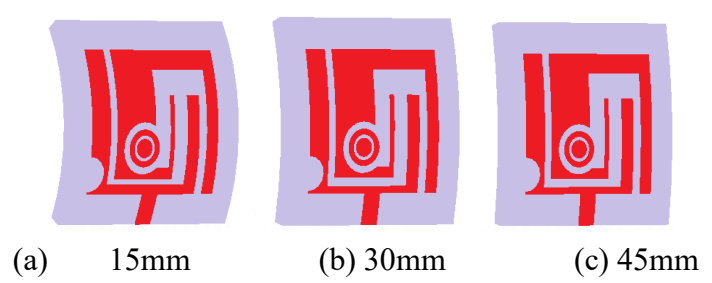


Fig 8:(a) Bending of the antenna at different radii along Y axis, (b) Bending of the antenna at different radii along X axis

The reflection coefficient variation with frequency for the antenna at different bending radii along Y axis and X axis are given in Figure 9 and figure 10 respectively. As can be seen from

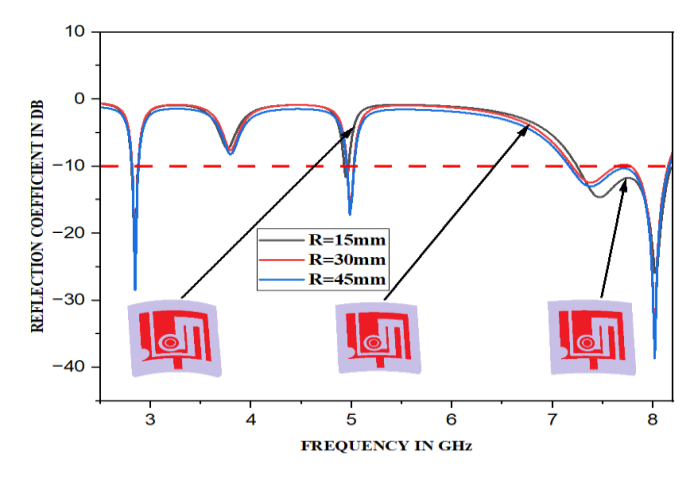


Fig 9: Reflection coefficient curve for various bending radii along Y axis.

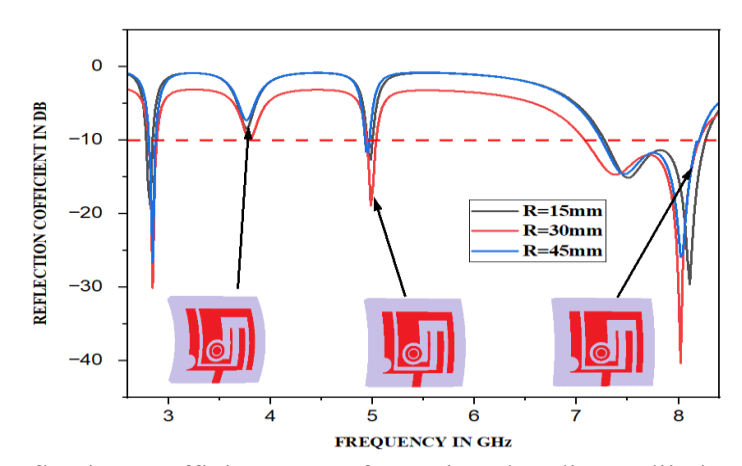


Fig 10: Reflection coefficient curve for various bending radii along X axis.

These figures, despite the variation in bending radii, the antenna consistently maintains its operating frequency points. The detailed resonance frequencies and operating bands when antenna is bent along Y axis are as follows: At a bending radius of 45 mm, the antenna resonates at 2.8 GHz, 4.9 GHz and a frequency band ranging from 7.18 GHz to 8.15 GHz. At 30mm, the

ISSN: 1311-1728 (printed version); ISSN: 1314-8060 (on-line version)

same frequency points are maintained and the frequency band slightly shifted to is 7.21GHz to 8.13 GHz. At 15mm, the antenna continues to resonate at 2.8 GHz and 4.9 GHz along with a band from 7.25 GHz to 8.2 GHz. Similarly, for bending along X axis the operating frequency bands are as follows: At 45mm, resonance is observed at 2.8 GHz and 4.9 GHz along with a frequency band of 7.25 GHz to 8.2 GHz. At 30mm, the resonance remains unchanged while the band slightly shifts to 7.09GHz to 8.2GHz. At 15mm, the frequency points stay the same and the band ranges from 7.27 GHz to 8.2 GHz. These results clearly indicate that the proposed antenna maintains stable resonance frequencies under both X and Y axis bending conditions with only minimum shifts in higher frequency bands. To assess the antenna's real-world performance, a prototype was fabricated and evaluated. Photographic evidence of the fabricated antenna and return loss measurement conducted using a virtual network analyser (VNA) are shown in figures 11(a) and 11(b) respectively.



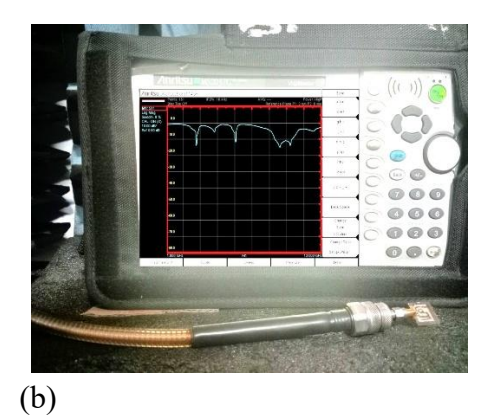


Figure 11:(a) Prototype of the antenna (b) Testing the protype

The return loss results obtained from both simulation and measurement are compared in figure 12. The outcomes show a maximum compatibility confirming the reliability of the simulation model.

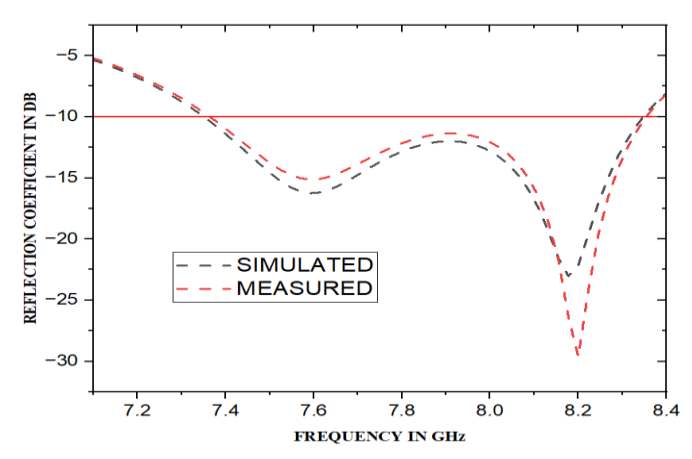


Figure 12: Comparison of Simulated Vs measured reflection coefficient of the proposed model

ISSN: 1311-1728 (printed version); ISSN: 1314-8060 (on-line version)

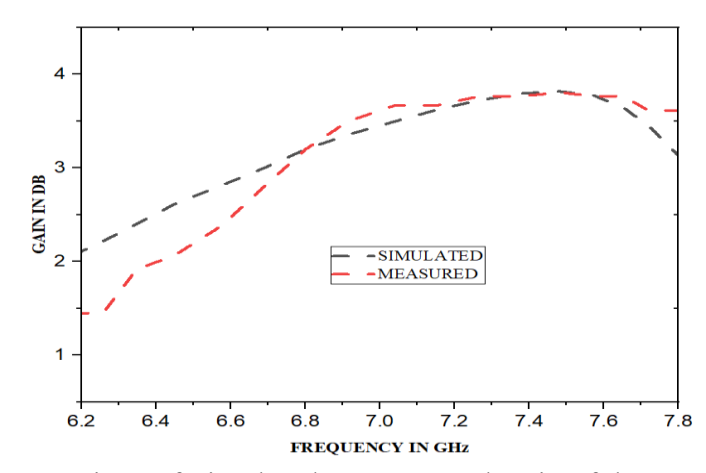


Figure 13: Comparison of Simulated Vs measured Gain of the proposed model

Figure 13 illustrates the comparison between simulated and measured gain the proposed antenna model. The results indicate that the antenna achieves a peak gain of 3.8 db. The deformation of the fabricated prototype under bending along Y axis and X axis is shown in figures 14(a) and 14(b) respectively.

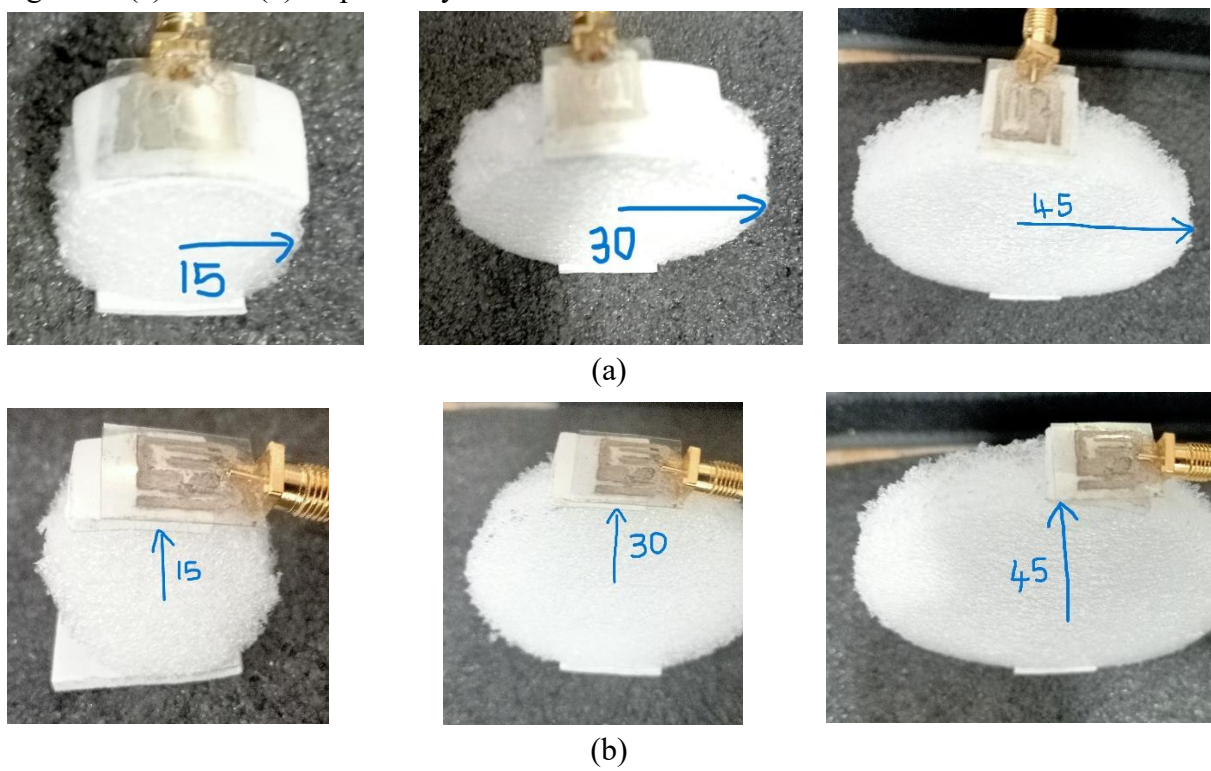


Figure 14: (a) Bending along Y axis, (b) Bending along X axis

The prototype of the proposed model can be easily bent horizontally and vertically at different radii as observed from figure 13.

Volume 38 No. 1s, 2025

ISSN: 1311-1728 (printed version); ISSN: 1314-8060 (on-line version)

IV. Comparison with Other Transparent Antennas

A comparative analysis is presented in Table 2 between the proposed final antenna and previously presented transparent antenna designs. The investigation clearly displayed that this transparent model delivers competitive performance all while maintaining a compact footprint.

REF	FOOT	OPERA	η%	GAI	FEED	SUBSTRATE	FLEXIBILI
	PRINT	TING		N			TY
		FREQU					
		ENCY					
17	50 X 50	2.4-2.5	42.6	2.63	LINE	ACRYL	-
	X 1		9				
21	30 X 20	2.7-5.8	41	0.53	SMA	MELINEX	YES
22	100 X 80	5	33.2	1.72	PROX	BOROSILICATE	-
			7		IMITY		
					COUP		
					LING		
24	90 X 60	2.3	NA	3.16	-	GLASS	-
	X 2						
26	150 X	800MHz	NA	-4.10	SMA	GLASS	-
	150						
27	75 X 50	2.15	44	2.57	COAX	PET	-
					IAL		
28	-	-	69.9	2.67	ACPS	LCP	-
31	120 X 60	2.2	68	0	CPW	GLASS	-
32	1000 x	5	33.2	1.72	LINE	BOROSILICATE	-
	800		7			GLASS	
33	38 X 13	2.95	NA	0.8	-	PDMS	YES
	X 1.5						
THIS	16 X 16	2.8	69.9	3.8	LINE	PET	YES
WOR		4.9					
K		7.3-8.3					

Table 2: Performance comparison of proposed model Vs existing transparent antennas

IV. Conclusion

An ultra-thin transparent triple band antenna is designed for operation at $2.8 \, \text{GHz}$, $4.9 \, \text{GHz}$ and within the range $7.3 \, \text{GHz} - 8.3 \, \text{GHz}$, effectively covering sub 6 and C band frequency ranges. This designed model achieves a $3.8 \, \text{dB}$ highest recorded gain and while maintaining 69.9% radiation efficiency. Further it has been subjected to bending analysis and the results were consistent with those of flat antenna. The antenna is fabricated on one side ITO coated PET sheet of dimensions $16 \, \text{x} \, 16 \, \text{mm}^2$ and tested using Virtual network analyser. Good agreement

Volume 38 No. 1s, 2025

ISSN: 1311-1728 (printed version); ISSN: 1314-8060 (on-line version)

is shown in conducted simulated and measured values of reflection coefficient and gain, confirming its consistency and overall reliability of the antenna's performance. Owing to its compact form and effectiveness, it stands as a suitable candidate for sub 6 GHz and C band use.

References

- [1] M. Alibakhshikenari et al., "Dual-Polarized Highly Folded Bowtie Antenna with Slotted Self-Grounded Structure for Sub-6 GHz 5G Applications," in IEEE Transactions on Antennas and Propagation, vol. 70, no. 4, April 2022, pp. 3028-3033 doi: 10.1109/TAP.2021.3118784.
- [2] C. White and H. R. Khaleel, "Chapter 3—Flexible Optically Transparent Antennas," in Innovation in Wearable and Flexible Antennas (WIT Transactions on State-of-the-Art in Science and Engineering), vol. 82. Southampton, U.K.: WIT Press, 2015, pp. 59–70.
- [3] Y. Morimoto, S. Shiu, I. W. Huang, E. Fest, G. Ye and J. Zhu, "An Optically Transparent Antenna on Glasses for 2.4GHz WiFi," 2023 IEEE International Symposium on Antennas and Propagation and USNC-URSI Radio Science Meeting (USNC-URSI), Portland, OR, USA, 2023, pp. 1555-1556, doi: 10.1109/USNC-URSI52151.2023.10238309.
- [4] Q. H. Dang, N. Nguyen-Trong, T. Kaufmann, T. Saarnimo, C. Hide and C. Fumeaux, "Dual-Band Circularly-Polarized Transparent GNSS Antenna for Vehicular Applications," in *IEEE Open Journal of Antennas and Propagation*, vol. 6, no. 1, pp. 201-211, Feb. 2025, doi: 10.1109/OJAP.2024.3487764.
- [5] Trujillo-Flores, J.I.; Torrealba-Meléndez, R.; Muñoz-Pacheco, J.M.; Vásquez-Agustín, M.A.; Tamariz-Flores, E.I.; Colín-Beltrán, E.; López-López, M. "CPW-Fed Transparent Antenna for Vehicle Communications". *Appl. Sci.* **2020**, *10*, 6001. https://doi.org/10.3390/app10176001D.
- [6] A. Gharaati, M. S. Ghaffarian and R. Mirzavand, "Transparent Wideband Circularly Polarized GNSS Antenna for Vehicular Applications," in *IEEE Access*, vol. 9, pp. 130185-130198, 2021, doi: 10.1109/ACCESS.2021.3113899.
- [7] D. Jang, N. K. Kong and H. Choo, "Design of an On-Glass 5G Monopole Antenna for a Vehicle Window Glass," in IEEE Access, vol. 9, pp. 152749-152755, 2021, doi: 10.1109/ACCESS.2021.3125977.
- [8] W. An, L. Xiong, S. Xu, F. Yang, H. -P. Fu and J. -G. Ma, "A Ka-Band High-Efficiency Transparent Reflect Array Antenna Integrated with Solar Cells," in *IEEE Access*, vol. 6, pp. 60843-60851, 2018, doi: 10.1109/ACCESS.2018. 2875359.Y
- [9] Y. -S. Chen, Y. -H. Wu and C. -C. Chung, "Solar-Powered Active Integrated Antennas Backed by a Transparent Reflect array for CubeSat Applications," in *IEEE Access*, vol. 8, pp. 137934-137946, 2020, doi: 10.1109/ACCESS.2020.3012133.
- [10] Rohaninezhad, M., Jalali Asadabadi, M., Ghobadi, C. *et al.* "Design and fabrication of a super-wideband transparent antenna implanted on a solar cell substrate". *Sci Rep* **13**, 9977 (2023). https://doi.org/10.1038/s41598-023-37073-5
- [11] S. Zarbakhsh, M. Akbari, M. Farahani, A. Ghayekhloo, T. A. Denidni and A. -R. Sebak, "Optically Transparent Subarray Antenna Based on Solar Panel for CubeSat

Volume 38 No. 1s, 2025

ISSN: 1311-1728 (printed version); ISSN: 1314-8060 (on-line version)

- Application," in *IEEE Transactions on Antennas and Propagation*, vol. 68, no. 1, pp. 319-328, Jan. 2020, doi: 10.1109/TAP.2019.2938740.
- [12] M. Salik, J. Ali, M. Uzair, A. Matthew and S. Chalermwisutkul, "Transparent UHF-RFID Tag Antenna for IoT Applications," 2024 21st International Conference on Electrical Engineering/Electronics, Computer, Telecommunications and Information Technology (ECTI-CON), Khon Kaen, Thailand, 2024, pp. 1-6, doi: 10.1109/ECTI-CON60892.2024.10594783.
- [13] R. B. V. B. Simorangkir *et al.*, "Transparent Epidermal Antenna for Unobtrusive Human-Centric Internet of Things Applications," in *IEEE Internet of Things Journal*, vol. 11, no. 1, pp. 1164-1174, 1 Jan.1, 2024, doi: 10.1109/JIOT.2023.3288994.
- [14] Y. Koga and M. Kai, "A Transparent Double Folded Loop Antenna for IoT Applications," 2018 IEEE-APS Topical Conference on Antennas and Propagation in Wireless Communications (APWC), Cartagena, Colombia, 2018, pp. 762-765, doi: 10.1109/APWC.2018.8503801.
- [15] S. Jamwal, S. Gupta, Z. A. P. Zibran, K. R. Jha and C. Singh, "An Optically Transparent Antenna for IoT Applications," *2020 International Conference on Electrical and Electronics Engineering (ICE3)*, Gorakhpur, India, 2020, pp. 696-698, doi: 10.1109/ICE348803.2020.9122979.
- [16] Desai A, Upadhyaya T, Patel J, Patel R, Palandoken M. Flexible CPW fed transparent antenna for WLAN and sub-6 GHz 5G applications. *Microw Opt Technol Lett.* 2020; 62: 2090–2103. https://doi.org/10.1002/mop.32287
- [17] S. Hong, Y. Kim and C. Won Jung, "Transparent Microstrip Patch Antennas with Multilayer and Metal-Mesh Films," in *IEEE Antennas and Wireless Propagation Letters*, vol. 16, pp. 772-775, 2017, doi: 10.1109/LAWP.2016.2602389.
- [18] Cai, L. An On-Glass Optically Transparent Monopole Antenna with Ultrawide Bandwidth for Solar Energy Harvesting. *Electronics* **2019**, *8*, 916. https://doi.org/10.3390/electronics8090916.
- [19] M. R. Haraty, M. Naser-Moghadasi, A. A. Lotfi-Neyestanak and A. Nikfarjam, "Improving the Efficiency of Transparent Antenna Using Gold Nanolayer Deposition," in *IEEE Antennas and Wireless Propagation Letters*, vol. 15, pp. 4-7, 2016, doi: 10.1109/LAWP.2015.2424918.
- [20] S. Hong, S. H. Kang, Y. Kim and C. W. Jung, "Transparent and Flexible Antenna for Wearable Glasses Applications," in *IEEE Transactions on Antennas and Propagation*, vol. 64, no. 7, pp. 2797-2804, July 2016, doi: 10.1109/TAP.2016.2554626.
- [21] A. Desai, M. Palandoken, J. Kulkarni, G. Byun and T. K. Nguyen, "Wideband Flexible/Transparent Connected-Ground MIMO Antennas for Sub-6 GHz 5G and WLAN Applications," in *IEEE Access*, vol. 9, pp. 147003-147015, 2021, doi: 10.1109/ACCESS.2021.3123366.
- [22] Sheikh, S., Shokooh-Saremi, M., & Bagheri-Mohagheghi, M. M. (2015). Transparent microstrip antenna made of fluorine doped tin oxide: a comprehensive study. *Journal of*

Volume 38 No. 1s, 2025

ISSN: 1311-1728 (printed version); ISSN: 1314-8060 (on-line version)

- *Electromagnetic Waves and Applications*, 29(12), 1557–1569. https://doi.org/10.1080/09205071.2015.1050528.
- [23] Y. Shi and W. J. Wang, "A Transparent Wideband Dual-Polarized Antenna for Sub-6 GHz Application," in *IEEE Antennas and Wireless Propagation Letters*, vol. 21, no. 10, pp. 2020-2024, Oct. 2022, doi: 10.1109/LAWP.2022.3188811
- [24] Azini, Alyaa & Kamarudin, M.R. & Abd Rahman, Tharek & Iddi, Hashim & Abdulrahman, Yusuf & Jamlos, Mohd. (2013). Transparent Antenna Design for WiMAX Application. Progress In Electromagnetics Research. 138. 133-141. 10.2528/PIER13021809.
- [25] C.-T. Lee, C.-M. Lee and C.-H. Luo, "The Transparent Monopole Antenna for WCDMA and WLAN," 2006 IEEE Annual Wireless and Microwave Technology Conference, Clearwater Beach, FL, USA, 2006, pp. 1-3, doi: 10.1109/WAMICON.2006.351948.
- [26] Colombel F. Castel X. Himdi M. Legeay G. Vigneron S. Motta Cruz E., "Ultrathin metal layer, ITO film and ITO/Cu/ITO multilayer towards transparent antenna", IET Science, Measurement & Technology ,2009, pp. 229 234, vol 3 doi: 10.1049/iet-smt:20080060.
- [27] G. Montisci, G. Mura, G. Muntoni, G. A. Casula, F. P. Chietera and M. Aburish-Hmidat, "A Curved Microstrip Patch Antenna Designed from Transparent Conductive Films," in *IEEE Access*, vol. 11, pp. 839-848, 2023, doi: 10.1109/ACCESS.2022.3233471.
- [28] M. Kim *et al.*, "Antenna-on-Display Concept on an Extremely Thin Substrate for Sub-6 GHz Wireless Applications," in *IEEE Transactions on Antennas and Propagation*, vol. 70, no. 7, pp. 5929-5934, July 2022, doi: 10.1109/TAP.2022.3161495.
- [29] J. Hautcoeur, A F. Colombel, A X. Castel, A M. Himdi, A E. Motta Cruz, "Optically transparent monopole antenna with high radiation efficiency manufactured with silver grid layer (AgGL)", 2009, Electronics Letters, 1014-1016, 45, doi:10.1049/el.2009.1218.
- [30] H. Qiu *et al.*, "Compact, Flexible, and Transparent Antennas Based on Embedded Metallic Mesh for Wearable Devices in 5G Wireless Network," in *IEEE Transactions on Antennas and Propagation*, vol. 69, no. 4, pp. 1864-1873, April 2021, doi: 10.1109/TAP.2020.3035911.
- [31] H. J. Song, T. Y. Hsu, D. F. Sievenpiper, H. P. Hsu, J. Schaffner and E. Yasan, "A Method for Improving the Efficiency of Transparent Film Antennas," in *IEEE Antennas and Wireless Propagation Letters*, vol. 7, pp. 753-756, 2008, doi: 10.1109/LAWP.2008.2008107.
- [32] Sheikh, S., Shokooh-Saremi, M., & Bagheri-Mohagheghi, M. M. (2015). Transparent microstrip antenna made of fluorine doped tin oxide: a comprehensive study. *Journal of Electromagnetic Waves and Applications*, 29(12), 1557–1569. https://doi.org/10.1080/09205071.2015.1050528.
- [33] L. Zhu, P.-Y. Chen and C. Zhang, "High-Performance, Transparent and Flexible Antenna Based on Conductive Nanocomposites," 2020 IEEE International Symposium on Antennas and Propagation and North American Radio Science Meeting, Montreal, QC, Canada, 2020, pp. 1491-1492, doi: 10.1109/IEEECONF35879.2020.9330137.